New electrochemical cell for *in situ* tunneling microscopy, cyclovoltammetry, and optical measurements

W. Schindler[a] and J. Kirschner
Max-Planck-Institut für Mikrostrukturphysik, Weinberg 2, 06120 Halle, Germany

(Received 21 March 1996; accepted for publication 14 June 1996)

We present a new electrochemical cell design, which enables *in situ* tunneling microscopy (STM), cyclic voltammetry, and optical measurements in a single setup and at the same surface area of the substrate. The design is compatible with the Nanoscope III system and allows the deposition and investigation of metal films down to the submonolayer range. We show *in situ* STM of the Cu(001) surface, cyclic voltammetry of the deposition of ultrathin Co films on Cu(001) from an aqueous $Na_2SO_4/CoSO_4$ solution and *in situ* magnetization measurements by magneto-optical Kerr effect on these Co films in the monolayer range. © *1996 American Institute of Physics.* [S0034-6748(96)06409-X]

I. INTRODUCTION

The *in situ* investigation of thin film growth and physical properties on a single sample is desirable to achieve detailed and reliable correlations between structure/morphology and physical, optical, magnetic, and electrochemical properties of electrodeposited films. However, STM investigations in electrochemical environment so far (for example, Refs. 1 and 2) are hardly compatible with other measurement techniques, which would probe the physical properties of the electrodeposits. Second, there are very few detailed studies in the literature on electrodeposited ultrathin magnetic films in the monolayer (ML) range. Since electrodeposition allows an inexpensive and fast film production, those studies seem to be of technological interest, in particular for mass storage applications[3] or possible applications of giant magnetoresistance.[4,5]

Electrochemical cells used for investigations in scanning tunneling (STM) and atomic force microscopes (AFM) (commercial and custom built cells) usually provide only up to a several hundred μl of electrolyte.[6–8] The small cell volume cannot be effectively degassed from oxygen,[9] which causes in the range of negative cell potentials (with respect to the standard calomel electrode, SCE) a cell current of up to three orders of magnitude higher than achievable in standard electrochemical cells ($\sim$0.1 $\mu A/cm^2$).[1] For this reason (sub-) monolayer deposition of less noble metals at potentials lower than 0 V cannot be resolved in the cyclovoltammogramm (current–voltage characteristics). Furthermore, the transport of ions is influenced by the small cell volume. The deposition depends on the concentration of the active ions in the liquid and the rapid evaporation of the electrolyte results in a nonconstant volume over time, which limits the time available for experiments.

Optical properties of the surface of electrochemically deposited films have been studied so far separately from STM by *in situ* x-ray scattering/absorption[10–15] or IR/Fourier transform infrared (FTIR) spectroscopy.[16,17] For these techniques a variety of special thin layer cell geometries combined with highly x-ray and infrared transparent windows has been developed, which is advantageous due to the absorption of x rays and infrared radiation in water, however hardly compatible with STM. The study of surface second harmonic generation (SHG)[18] or surface enhanced Raman spectroscopy (SERS)[19–23] at electrochemical interfaces would not necessarily require a thin layer cell geometry with reduced electrochemical versatility.

This is also the case for the *in situ* study of other optical properties of electrochemically deposited films in the range of visible light. These measurements require the stability of the deposited films during the time of the optical measurement, in particular for investigations on ultrathin films consisting of only a few atomic layers. This time may be up to 10 min in the case of magnetization measurements by magneto-optical Kerr effect (MOKE) given as an example below. The stable conditions are desirable on a macroscopic area of $\sim$1 mm^2, which corresponds to the area of a typical unfocused laser spot on the sample. However, this is by a factor of 10^4 larger than the area measurable by STM. Therefore, the *in situ* cyclic voltammetry is essential to control the film deposition and dissolution as well as its stability during the optical measurements with submonolayer accuracy.

In the following, we present an electrochemical cell design, which enables the combination of different measurement techniques together with STM.

II. CELL DESIGN

The electrochemical cell (Fig. 1) is manufactured completely out of quartz since this material is most inert against ultrapure water and acids. The cell provides a number of necks, which are constructed as standard female joints, similar to those commonly used for chemical equipment. The various measurement facilities and connections are inserted into these joints and therefore easily changeable. A 60/46 male joint [Fig. 1(4)] closes the cell at the top against the air and provides the housing for the STM scanner head as described below.

The electrolyte volume is $\sim$100 ml, which results in stable concentrations of the electrolyte solution during the whole experiment for several hours. The cell provides a stan-

[a]Electronic mail:schi@mpi-msp-halle.mpg.de

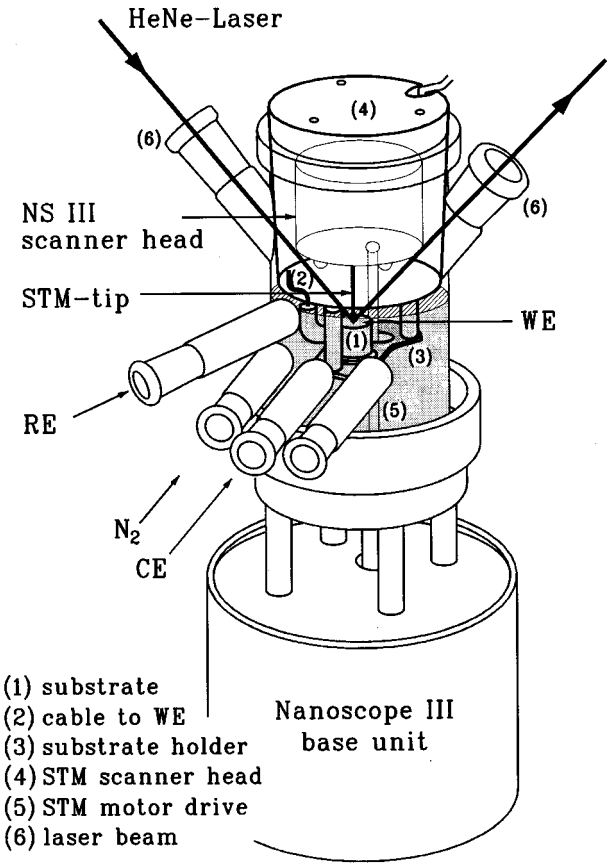

FIG. 1. Schematic drawing of the electrochemical cell, fitting onto the standard Nanoscope III (NS III) ECSTM base unit. The adjustment plate of the scanner head and the glass tubes for the laser beam are not drawn as well as the pole shoes of the electromagnet. The direction of the magnetic field is parallel to the plane of the laser beam. It can be rotated in this plane to measure longitudinal and polar MOKE. The sample is the working electrode (WE); counter (CE), and reference (RE) electrode as well as the nitrogen gas (N_2) are connected to the cell using joints. The level of the electrolyte (dashed area) is adjusted a few millimeters above the surface of WE.

dard four electrode design with the working electrode (WE), counter electrode (CE), reference electrode (RE), and the STM tip.

The WE is a single crystal or another substrate with a diameter of several millimeters. It is mounted on a special 14/23 male joint [Fig. 1(1)], which encloses all areas of WE except the surface. The polished and oriented surface of WE points upwards, as is required by our STM. The remaining free gap between WE and the surrounding glass is carefully isolated against the electrolyte using a commercial lacquer. The electrical contact to WE is made by a miniature coaxial cable [Fig. 1(2)], which leads inside a glass tube (and thereby protected from the electrolyte) to the backside of WE into the 14/23 joint. This module is easily changeable and sticks in a corresponding female joint on a special holder [Fig. 1(3)], which is mounted ~15 mm below the bottom of the 60/46 male joint. The counter electrode (CE) is made out of a platinum wire and is connected to the cell volume by a frit to prevent pollution of the electrolyte. A standard calomel electrode (SCE) is used as reference electrode. The potential at WE is measured by a Luggin capillary ending about 1 mm in front of the surface of WE. The cell potential is applied between WE and CE. The cell can be operated using the standard Nanoscope III bipotentiostat, as well as using standard electrochemical equipment and potentiostats.

The level of the electrolyte is adjusted several millimeters above the surface of WE as indicated by the dashed area in Fig. 1. This provides a large volume around the sample/WE, which minimizes the limits to the diffusion of species to and from the confined region around WE. The electrolyte is directly degassed with ultrapure nitrogen or argon gas using a miniature frit as inlet into the electrolyte.

The standard 0.7 or 12 μm STM scanner heads of the Nanoscope III are mounted inside the abovementioned 60/46 male joint [Fig. 1(4)]. The sample holder [Fig. 1(3)] is mounted at the bottom of this joint [Fig. 1(4)] as described above, so that sample and STM form a unit, which can be removed or inserted into the cell as a whole. This close connection as well as the use of quartz reduces the thermal drift between sample and STM tip. The scanner head is mounted inside the 60/46 joint on an adjustment plate, which provides the coarse positioning of the STM tip. Any undesired movement of the mechanics is prevented by springs, which brace the plate against the 60/46 joint. The fine engagement of the STM tip is realized according to the standard Nanoscope technique and using the standard motor drive of the Nanoscope III base unit. The motor axis [Fig. 1(5)] leads through the cell inside a glass tube (not drawn in Fig. 1), which prevents the contact to the electrolyte.

Two female joints at 45° to the surface normal of WE [Fig. 1(6)] provide direct access for optical measurements. Two changeable glass tubes fit into these joints and lead close to the surface of WE. The end of each tube is sealed by a 0.1 mm thin glass plate of optical quality, perpendicular to the incident and reflected (at the surface of WE) laser beam. It dips completely into the electrolyte. This avoids the penetration of the laser beam through the free surface of the liquid as well as undesired refraction of the laser beam and minimizes possible effects of the electrolyte on the measurement by minimizing the path of the laser beam through the solution. The total path length through the electrolyte is typically 10 mm. It can be reduced to below 1 mm simply by changing the geometry and/or the glass tubes which dip into the electrolyte. The optical measurements can be done simultaneously with STM and cyclic voltammetry at the STM tip position.

The adjustments of the STM tip and the laser beam are controlled using a long distance microscope with CCD camera and monitor.

The cell fits in between the pole shoes of an external electromagnet to perform magnetization measurements on the deposited films. The magnet is rotatable around the cell and allows parallel and perpendicular orientation of the magnetic field to the sample surface. The maximum field values at the sample are ~0.5 T.

Due to this strong magnetic field and corresponding stray fields, each part of the electrochemical, the STM and the MOKE setup is machined out of nonmagnetic material to prevent any mechanical motion. Also for this reason, we use for the experiment a commercial vibration isolated table,

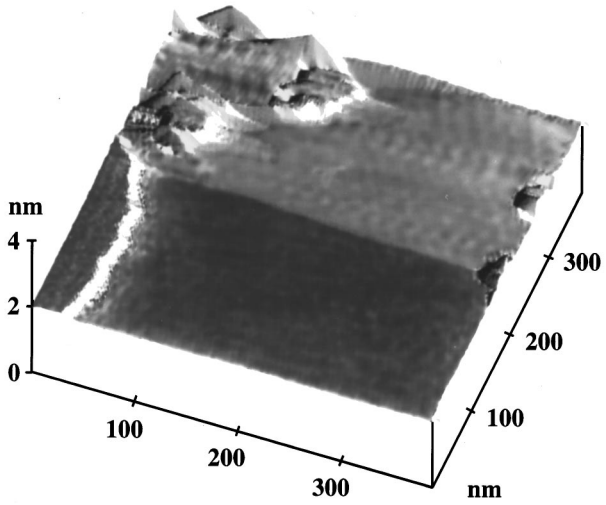

FIG. 2. STM measurement of a flat area of the Cu(001) surface before the deposition of Co. Monoatomic step (left-hand side) and atomically flat plateau with edge lengths up to 300 nm (foreground). Higher structures (up to 10 nm) and smaller plateaus as seen in the upper left-hand side corner are also usually observed on our Cu crystals. $U_{WE}=-270$ mV; $U_{bias}=275$ mV; $I_{tunnel}=3$ nA.

which is manufactured out of aluminum and granite. The electromagnet is mechanically decoupled from this table and from the experimental apparatus.

III. MEASUREMENTS AND PERFORMANCE

We tested the cell design using the deposition of ultrathin Co films on Cu(001) and present *in situ* magnetization measurements on electrodeposited Co films in the ML range.

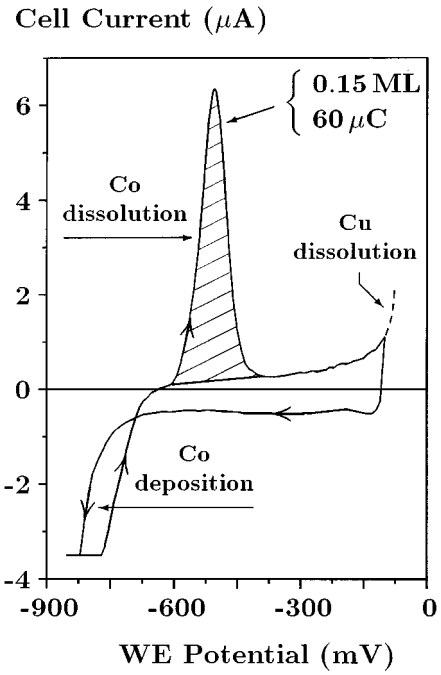

FIG. 3. Cyclovoltammogramm of the deposition of Co on Cu(001). The potential is ramped at 10 mV/s in the direction indicated by the arrows. The deposited charge (60 μC) corresponds to the integral of the anodic peak (dashed area). The estimation of the Co film thickness (0.15 ML) was done using the area of the crystal surface (0.8 cm^2) and the bulk-Co lattice constant (0.351 nm). The dissolution of the Cu crystal starts at a WE potential of -130 mV. Potentials are with respect to SCE.

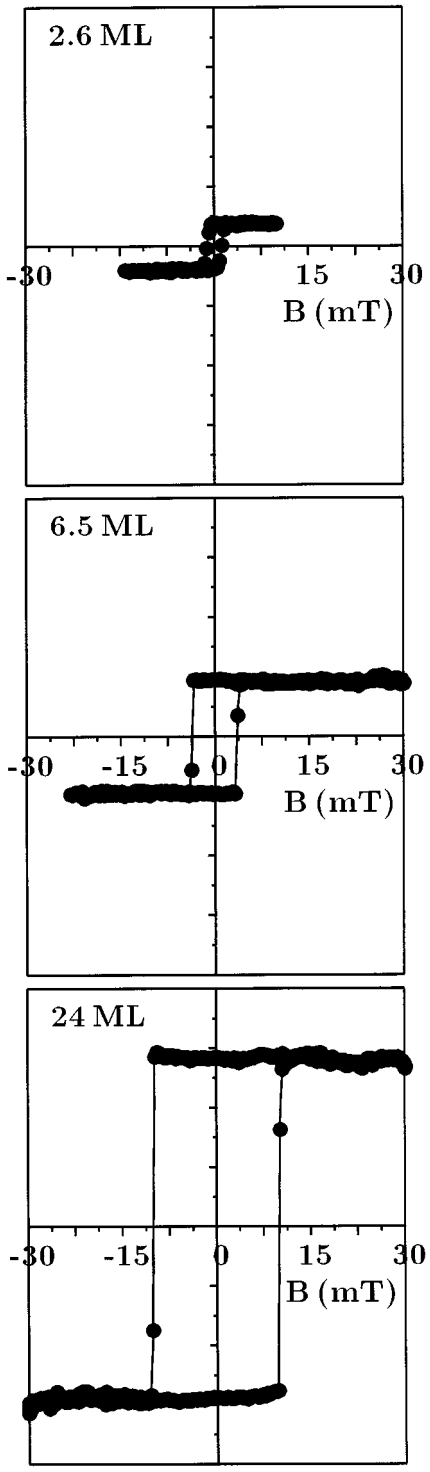

FIG. 4. Longitudinal MOKE measurements of 2.6, 6.5, and 24 ML Co on Cu(001). The measurement time per hysteresis loop was ~20 s. The temperature during Co deposition and MOKE measurements was 295 K. The Co thickness was determined from the anodic peak area in the cyclovoltammogramm as shown in Fig. 3. All graphs have the same vertical and horizontal scales.

The Cu(001) single crystal (WE) was oriented to better than 0.2° deviation and mechanically polished using 0.25 μm diamond paste in the final step. Afterwards the crystal was annealed at 700 °C in an Ar/H_2 mixture for 5 h. Then it was mounted on the above described sample holder and care-

fully isolated against the surrounding liquid using a commercial lacquer (Miccroshield, Hi-Tek Products Ltd., UK). Finally it was electrochemically polished in 65% H_3PO_4 at $+1.8$ to $+2.4$ V (against a carbon electrode) for several minutes. The crystal was then transferred into the cell under protection of ultrapure water (Milli-Q plus) to prevent any contact to air. The cell has been cleaned before each experiment using a mixture of concentrated H_2SO_4/H_2O_2 and subsequently sterilized in ultrapure water. The measurements were performed in an aqueous electrolyte of 0.3 M Na_2SO_4 and 1 mM $CoSO_4$. STM tips have been electrochemically etched from tungsten wire of 0.25 or 0.5 mm diameter and have been isolated by Apiezon wax. Typical residual faradaic currents were less than 0.5 nA at tip potentials between -400 mV and -100 mV versus SCE.

The STM performance of our cell is demonstrated in Fig. 2. The surface structure of the Cu(001) single crystal was measured under potentiostatic control at a WE potential of -270 mV using the standard Nanoscope III bipotentiostat. Well-prepared surfaces show atomically flat plateaus with edge lengths of up to 300 nm and steps of single to several ML height (Fig. 2). However, we often find higher structures and smaller flat areas as is also seen in the upper left-hand corner of Fig. 2. The overall roughness averaged laterally over 1 μm^2 depends on the crystal preparation procedure. It has been found to be less than 10 nm after alternating electrochemical etching at $+1.8$ V and $+2.4$ V and after the removal of $\sim$0.2–0.5 mm from the ''as-polished'' Cu(001) surface. The detailed surface structure may also depend on the pH value of the electrolyte, which has been held constant at pH$\approx$5 in all measurements.

The cyclovoltammogramm of the Co deposition is shown in Fig. 3. It was recorded using a standard electrochemical equipment (potentiostat: HEKA GmbH; SCE: Schott–Geräte GmbH) with our cell. The potential of WE was cycled between -120 mV and -860 mV at 10 mV/s, as indicated by the arrows in Fig. 3. Co on Cu(001) does not show an underpotential deposition (UPD) but only the usual bulk deposition. The Co deposition starts at a WE potential of -750 mV. The integral of the anodic peak (dashed area in Fig. 3) during the following increase of the WE potential represents the equivalent charge related to the dissolution of the previously deposited Co film. The anodic peak area in Fig. 3 corresponds to a coverage of 0.15 ML Co as calculated from the area of the single crystal of 0.8 cm^2 and the bulk-Co lattice constant of 0.351 nm. The achievable resolution of the charge measurement is $\sim$0.02 ML. Limits to the diffusion to and from the region around WE cannot be observed due to the low currents during the deposition/dissolution of films in the ML range (see Fig. 3).

MOKE measurements at the STM tip position were performed at a wavelength of 632.8 nm using a 1 mW HeNe laser and a lock-in modulation technique.[24] The magnetic field for the measurement was adjusted in-plane parallel to the crystal surface (longitudinal MOKE). The Co films were held in a stable condition during the measurement time of $\sim$5 min by adjusting the WE potential to -650 mV (no current to or from WE, see Fig. 3). The dissolved charge after 5 min was within 0.1 ML the same as it was measured by cyclic voltammetry if dissolving the Co films immediately after the deposition. A set of typical magnetic hysteresis loops of 2.6, 6.5, and 24 ML Co on Cu(001) is shown in Fig. 4. The magnetization of these films is parallel to the Cu(001) surface (in-plane). The orientation within the (001) plane is random. This is in agreement with MOKE measurements on MBE deposited ultrathin Co films in the same thickness range.[25] The coercive field of the Co films increases with thickness from 0.9 mT at 2.6 ML to 10 mT at 24 ML, significantly higher than it is known from best MBE films[25] prepared on Cu(001) substrates, which show atomically flat plateaus of several hundred nm edge lengths over large areas of μm scale. We attribute this higher coercivity of the electrochemically deposited films to the different preparation of the Cu(001) substrate. This is supported by STM measurements, which show fewer and smaller atomically flat plateaus and (the abovementioned) enhanced roughness on μm scale, compared to that observed on UHV-prepared crystals. The resolution of the MOKE measurement as derived from the noise level in Fig. 4 is $\sim$0.2 ML.

ACKNOWLEDGMENTS

The authors would like to thank D. M. Kolb and M. Hölzle from the Electrochemical Department of the University of Ulm (Germany) as well as W. Schwarzacher from H. H. Wills Laboratory of the University of Bristol (UK) for their support in the initial stages of the work. We are grateful to H. Menge of our institute for the preparation of the Cu single crystals.

[1] D. M. Kolb, R. J. Nichols, and R. J. Behm, in *Electrified Interfaces in Physics, Chemistry and Biology*, edited by R. Guidelli (Kluwer Academic, Dordrecht, 1992), p. 275.
[2] W. Obretenov, M. Höpfner, W. J. Lorenz, E. Budevski, G. Staikov, and H. Siegenthaler, Surf. Sci. **271**, 191 (1992).
[3] T. M. Harris, G. M. Whitney, and I. M. Croll, J. Electrochem. Soc. **142**, 1031 (1995).
[4] M. Alper, K. Attenborough, R. Hart, S. J. Lane, D. S. Lashmore, C. Younes, and W. Schwarzacher, Appl. Phys. Lett. **63**, 2144 (1993).
[5] K. D. Bird and M. Schlesinger, J. Electrochem. Soc. **142**, L65 (1995).
[6] H. Siegenthaler, in *Scanning Tunneling Microscopy II*, edited by R. Wiesendanger and H. J. Güntherodt (Springer, Berlin, 1992), p. 7.
[7] E. J. Wanless, T. J. Senden, A. M. Hyde, and T. J. Sawkins, Rev. Sci. Instrum. **65**, 1019 (1994).
[8] J. Wiechers, T. Twomey, D. Kolb, and R. J. Behm, J. Electroanal. Chem. **248**, 451 (1988).
[9] P. N. Ross, in *Structure of Electrified Interfaces*, edited by J. Lipkowski and P. N. Ross (VCH, New York, 1993), p. 38.
[10] G. J. Hansen and W. E. O'Grady, Rev. Sci. Instrum. **61**, 2127 (1990).
[11] H. D. Abruna, in *Electrochemical Interfaces*, edited by H. D. Abruna (VCH, New York, 1992), p. 1.
[12] Z. Nagy, H. You, and R. M. Yonco, Rev. Sci. Instrum. **65**, 2199 (1994).
[13] K. M. Robinson and W. E. O'Grady, Rev. Sci. Instrum. **64**, 1061 (1993).
[14] M. E. Herron, S. E. Doyle, K. J. Roberts, J. Robinson, and F. C. Walsh, Rev. Sci. Instrum. **63**, 950 (1992).
[15] J. Zegenhagen, G. Materlik, J. P. Dirks, and M. Schmäh, in *Synchrotron Techniques in Interfacial Electrochemistry* (Kluwer Academic, Dordrecht, 1994), p. 349.
[16] S. M. Stole, D. D. Popenoe, and M. D. Porter, in *Electrochemical Interfaces*, edited by H. D. Abruna (VCH, New York, 1992), p. 341.
[17] M. A. Rob, Rev. Sci. Instrum. **63**, 3636 (1992).
[18] G. L. Richmond, in *Electrochemical Interfaces*, edited by H. D. Abruna (VCH, New York, 1992), p. 267.
[19] S. L. F. A. da Costa, S. M. L. Agostinho, and J. C. Rubim, J. Electroanal. Chem. **295**, 203 (1990).
[20] B. H. Loo, Chem. Phys. Lett. **213**, 479 (1993).

[21] G. Niaura and A. Malinauskas, Chem. Phys. Lett. **207**, 455 (1993).
[22] H. Feilchenfeld and M. J. Weaver, J. Phys. Chem. **95**, 7771 (1991).
[23] K. Itoh, K. Minami, T. Tsujino, and M. Kim, J. Phys. Chem. **95**, 1339 (1991).
[24] S. D. Bader, J. Magn. Magn. Mater. **100**, 440 (1991).
[25] H. A. Wierenga, W. de Jong, M. W. J. Prins, Th. Rasing, R. Vollmer, A. Kirilyuk, H. Schwabe, and J. Kirschner, Phys. Rev. Lett. **74**, 1462 (1995).